 doi:10.20944/preprints202207.0058.v1

Article

Heparan Sulfate Facilitates Binding of hIFNγ to its Cell-Surface Receptor hIFNGR1

Elisaveta Miladinova [1], Elena Lilkova[2,*], Elena Krachmarova[3,*], Kristina Malinova[3], Peicho Petkov[1], Nevena Ilieva[2], Genoveva Nacheva[3] and Leandar Litov [1]

[1] Faculty of Physics, Sofia University "St. Kliment Ohridski"
[2] Institute of Information and Communication Technologies, Bulgarian Academy of Sciences
[3] Institute of Molecular Biology, Bulgarian Academy of Sciences
* Correspondence: elena.lilkova@iict.bas.bg (E.L.); elenakrachmarova@bio21.bas.bg (E.K.)

Abstract: The extremely controversial conclusions about the function of human interferon-gamma (hIFNγ) C-terminus as well as the lack of a consistent model explaining its role in the receptor binding prompted us to scrutinize the interaction of hIFNγ with its extracellular receptor hIFNGR1 in different scenarios by means of molecular dynamics simulations. We find that the two molecules alone fail to form a stable complex but the presence of heparan-sulfate-like oligosaccharides largely facilitates the process by both demobilizing the highly flexible C-termini of the cytokine and assisting in the proper positioning of its globule between the receptor subunits. An antiproliferative-activity essay on cells depleted from surface sulfation confirms qualitatively the simulation-based multistage complex-formation model. Our results reveal the key role of HS and its proteoglycans in all processes involving hIFNγ signalling.

Keywords: human interferon gamma; human interferon gamma receptor; receptor binding; heparan sulfate; co-receptor; molecular dynamics simulations; sodium chlorate; kynurenine antiproliferative assays; hIFNγ signalling

1. Introduction

Interferon-gamma (IFNγ) is the only known type II interferon [1]. It is secreted by the natural killer (NK) and natural killer T (NKT) cells as well as by the CD4 and CD8 cytotoxic T1 lymphocytes stimulated by various antigens, toxins and mitogens. IFNγ is one of the major macrophage stimulating factors. It shows multiple biological effects: increases antigen presentation and lysosome activity of macrophages and NK cells, suppresses Th2 cell activity, promotes Th1 cell differentiation, stimulates antiviral and antiparasitic cell activity, expresses general effects on cell proliferation, apoptosis, etc. Due to these functions, IFNγ is appropriate for treatment of viral, parasitic and immunological diseases (for review, see [2]).

Human interferon-gamma (hIFNγ) is a 17 kDa single protein consisting of 143 amino acids (aa), of which 28 are basic. It is organized in six α-helices (comprising 62% of the molecule), which are linked by short unstructured regions. Additionally, the cytokine contains a long unstructured C-terminal domain consisting of 21 aa, eight of which are Lys and Arg. Under physiological conditions hIFNγ is organized in a non-covalent homodimer, in which the two monomers are associated in antiparallel orientation [3].

hIFNγ is recognized by its own species-specific receptor (hIFNGR) [3]. The hIFNγ receptor is found on the surface of all human cells except for erythrocytes at concentrations of 500–20 000 receptors per cell [4]. The hIFNGR consists of two proteins – chain-1 (hIFNGR1) and chain-2 (hIFNGR2) [5]. The first one is responsible for ligand (hIFNγ) binding (K_d = 0.1–1 nM) and the second one is necessary for triggering the hIFNγ signal transduction pathway, resulting in the activation in the cell nucleus of over 200 different genes [1,6].

 doi:10.20944/preprints202207.0058.v1

The 3D structure of the free hIFNγ homodimer [7], as well as the hIFNγ in a complex with the soluble part of the hIFNGR1 receptor [8] are determined by X-ray crystallography. The receptor binding sites on each side of the hIFNγ molecule are located in three distinct areas: i) the loop between the first two N-terminal helices (residues 18–26) of one of the monomers, ii) His^{111}, and iii) a short putative area (residues 128–131) in the flexible C-terminal domain of the other monomer. However, the extensive structure-functional studies do not shed much light on the biological functions of the unstructured 21 aa long C-terminal tail of the hIFNγ, one reason for this being the lack of X-ray diffraction data for the last 21 C-terminal aa [7–9].

Three main strategies have been employed so far to study the structure-function relation of the C-terminal part of hIFNγ: i) blocking of selected areas by sequence specific monoclonal antibodies (MAB); ii) truncation of selected regions using sequence specific proteases; iii) deletion/substitution of one or more aminoacid residues by site directed mutagenesis. The conclusions drawn from all these studies (in terms of significance of the unstructured C-terminal domain) vary from "extremely important" to "totally dispensable".

The hIFNγ C-terminal region is highly positively charged, which makes it highly susceptible to proteases [10,11]. The basic amino acids are concentrated in two domains: the first one (denoted D1) encompasses amino acids ^{125}KTGKRKR^{131} and the second one (D2) includes the sequence ^{137}RGRR^{140}. The proteolytically sensitive segment D1 is assumed to greatly contribute to the high affinity binding of hIFNγ to the receptor and consequently to its capacity of triggering multiple cell responses [12–14]. Complete removal of the flexible C-terminus inactivates the cytokine. This, however, cannot explain the modulating effect of the length of the C-terminal tail on hIFNγ activity, i.e. the gradual increase in activity on removal of up to 9 C-terminal amino acids (which includes D2) and the subsequent decrease in biological activity following further deletions, which renders D1 functionally more important [15,16].

In a series of papers Lortat-Jacob et al. [17–19] described remarkable effects of the glycosaminoglycans (GAGs) heparin and heparan sulfate (HS) on the hIFNγ activity, physico-chemical properties and proteolytic processing of its C-terminal domain. HS is highly sulfated linear polymer of the disaccharide 4IdoAα/GlcAβ1-4GlcNα1, occurring as an integral component of the basement membrane of all mammalian cells [20,21]. Heparan sulfate proteoglycans (HSPGs) are cell-surface and secreted proteins consisting of a core domain to which long linear HS glycosaminoglycan chains are covalently attached [22]. It has been shown that hIFNγ binds to HS with high affinity [23]. Although hIFNγ bears four basic clusters (^{55}KLFKNFK^{61}, ^{86}KKKR^{89}, ^{125}KTGKRKR^{131} and ^{137}RGRR^{140} that could potentially function as HS binding sites, the specific interaction of the cytokine with HS is entirely related to the last two of them – D1 and D2 that are located within the C-terminus [24]. The binding constants (K_d) of hIFNγ to hIFNGR1 and HS are 10^{-10} M and 1.5×10^{-9} M respectively [19,23].

Here we report our computational studies on the interaction of hIFNγ with hIFNGR1 in different scenarios using molecular dynamics (MD) simulations. We aim to reveal the mechanism of this interaction and to clarify the role of the C-terminus in hIFNγ—hIFNGR1 binding. Based on our findings, we put forward the hypothesis that HSPGs act as co-receptors for the cytokine and facilitate its binding to its cellular receptor.

2. Materials and Methods

2.1. Molecular Dynamics Simulations

2.1.1. Input Structures

The 3D structures of hIFNγ and hIFNGR1 were extracted from the Protein Data Bank [25] under PDB ID 1FG9 [9]. The 1FG9 complex was used as input for the reference simulation of the hIFNγ—hIFNGR1 complex (Fig. 1a).

Preprints (www.preprints.org) | NOT PEER-REVIEWED | Posted: 5 July 2022 doi:10.20944/preprints202207.0058.v1

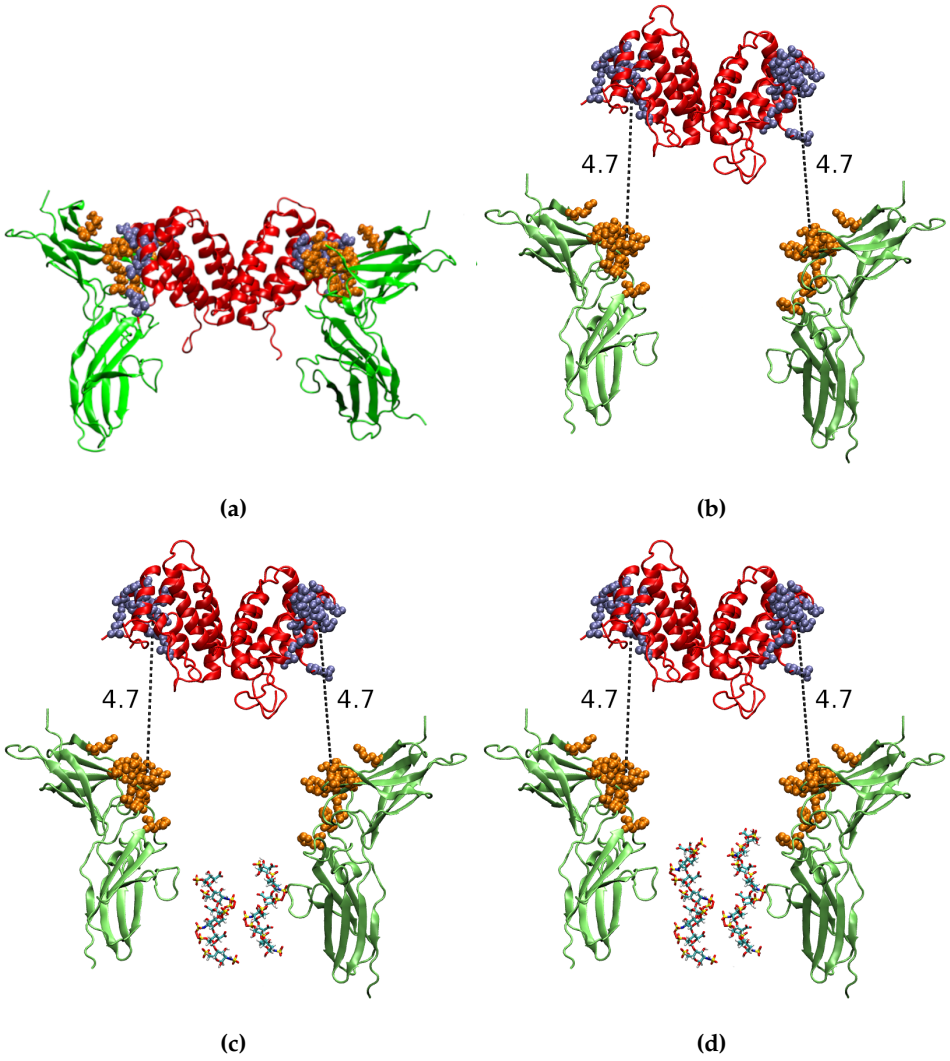

Figure 1. Initial models used to study the binding of hIFNγ to hIFNGR1 in different scenarios. (a) Reference simulation based on the crystallographic structure of the complex; (b) Binding of the full-length hIFNγ to its receptor; Binding of the full-length hIFNγ to its receptor in the presence of HS-derived (c) hexa- or (d) octasaccharides. The cytokine and the receptor subunits are presented in red or green cartoons respectively. The amino acid residues in the hIFNγ and hIFNGR1 molecules, participating in the binding, according to [9], are shown in blue and orange spheres. The HS-derived oligosaccharides are colored by atom type and presented as licorice.

To study the formation of the cytokine–receptor complex, a configuration was set up in which the hIFNγ molecule was translated a few nanometers along the z-axis to distance it from the two receptors (Fig. 1b). Since the 1FG9 structure does not provide information about the coordinates of the unstructured C-terminal domain, the last 18 missing aa residues were added to the protein structure, as described in [26,27]. In addition, the missing segment ^{141}EVDYDP^{146} in the hIFNGR1 molecules was reconstructed using the macromolecular model building toolkit Coot [28]. The last two C-terminal amino acid residues of the two hIFNGR1 molecules were constrained to mimic reduced flexibility due to membrane attachment of the receptors.

To investigate how HSPGs could influence the interaction between hIFNγ and its receptor, two models were built in which either two HS-derived hexa- (Fig. 1c) or two octasaccharides (Fig. 1d) were placed between the two receptor molecules. The 1HPN pdb entry [24] was used to develop structural models of HS-like chains with degree of degree of polymerization 6 (dp6) and 8 (dp8) respectively. The Glycan Reader and Modeler module [29] of the CHARMM-GUI server [30] was used for the generation of a three-dimensional

Preprints (www.preprints.org) | NOT PEER-REVIEWED | Posted: 5 July 2022 doi:10.20944/preprints202207.0058.v1

structure, corresponding to the chosen carbohydrate sequence, as well as a topology using the latest version of the CHARMM36 carbohydrate force field [31]. The topology was converted to a GROMACS-compatible topology using the parmed module of Ambertools 16 [32]. The first monosaccharide was constrained to model immobilization of the HS chains at the cell surface.

2.1.2. MD Simulation Protocol

All simulations were performed with the molecular dynamics simulation package GROMACS, version 2021.1 [33]. The protein was parameterized with the CHARMM36 protein force field [34] and the oligosaccharides – with the CHARMM36 carbohydrate force field [31]. The systems were solvated in rectangular boxes with a minimal distance to the box walls of 2 nm under periodic boundary conditions. Counterions were added to all systems to neutralize their net charge. The neutralized systems were energy minimized using the steepest descent method with a maximum force tolerance of 100 kJ/(mol nm). The minimized structures were equilibrated by a short 50 ps canonical simulation at a temperature of 310 K, followed by a 200 ps isothermal-isobaric simulation at a temperature of 310 K and a pressure of 1 atm with the Berendsen thermo- and barostat [35].

For the production MD simulations temperature and pressure were maintained by a v-rescale thermostat [36] with a coupling constant of 0.25 ps and a Parrinello-Rahman barostat [37,38] with a coupling constant of 1 ps. The leapfrog integrator [39] was used with a time-step of 2 fs, with constraints imposed on the bonds between heavy atoms and hydrogens with the help of the PLINCS algorithm [40]. Van der Waals interactions were smoothly switched off from a distance of 1.0 nm and truncated at 1.2 nm. Electrostatic interactions were treated using the smooth PME method [41] with a direct PME cut-off of 1.2 nm. Trajectory frames were recorded every 200 ps and the simulation had a duration of 650 ns.

2.2. Cell Culture and Treatment with Sodium Chlorate

WISH cell line (ATCC®CCL-25™) was propagated in Eagle's Minimum Essential Medium (EMEM,ATCC®30-2003™) supplemented with 10% fetal bovine serum (Gibco™) and sodium chlorate ($NaClO_3$, Sigma) to final concentration of 30 mM. $NaClO_3$ was used as a supplement throughout the whole experimental procedure in order to ensure the reduction of sulfation of heparan sulfate. $NaClO_3$ concentration (30 mM) was chosen based on literature data [42] and our experimental data on the cell proliferation rate performed by MTT assay (data not shown). Cells were cultured in 25 cm^2 flasks (ThermoScientific™ Nunc™) at 37°C incubator with 5% CO_2. After overnight incubation at 37°C and 5-6 % CO_2, the cells were trypsinised and re-plated with density of 1.5×10^6 per well on a 96-well plate (Corning®)in culture medium containing 30 mM $NaClO_3$. On the next day, the cells were treated with 15 ng/ml hIFNγ purified as described in [43]. Further, the antiproliferative activity of hIFNγ was measured by a modified kynurenine bioassay as described in [44].

3. Results

3.1. Molecular Modelling

To monitor the process of cytokine–receptor binding, we used the centre-of-mass (COM) distances between the receptor-binding sites in the molecule of hIFNγ and the cytokine–binding sites in the hIFNGR1 subunits (Fig. 1b), denoted d_1 and d_2. In the initial conformations of the binding simulations these quantities had a value of 4.7 nm. In the reference simulation of the complex d_1 had an average value of 6.87$\pm$0.56 nm, and d_2 = 6.58$\pm$0.24 nm.

The binding of the full-length hIFNγ and the two hIFNGR1 subunits does not lead to proper formation of the complex. The final configuration of this simulation is shown on Fig. 2a. The long unstructured and highly positively charged C-terminal tails of the two hIFNγ monomers extend downwards and move away from the globule of the cytokine to bind to two negatively charged protruding domains in the receptor subunits, which we refer to

Preprints (www.preprints.org) | NOT PEER-REVIEWED | Posted: 5 July 2022 doi:10.20944/preprints202207.0058.v1

as "knees" (Fig. 2c), located right next to the lower part of the cytokine-binding site. This keeps the globule at a distance of about 20-25 nm from the cytokine-binding sites on the hIFNGR1 molecules and prevents proper interaction of the two binding interfaces (Fig. 2b). This is also reflected in the contact maps between the two hIFNγ monomers (denoted chain A and B) and the two receptor subunits (denoted chain C and D), presented in Fig. 3 and 4.

The contact maps show the frequency of the close contacts between the two molecules. A contact is considered present, if any two heavy atoms of a hIFNγ monomer and a receptor subunit are within a cutoff radius of 4.5 Å. For this analysis, only the last 150 ns of each trajectory were employed. The contact maps were generated using the MDTraj package [45].

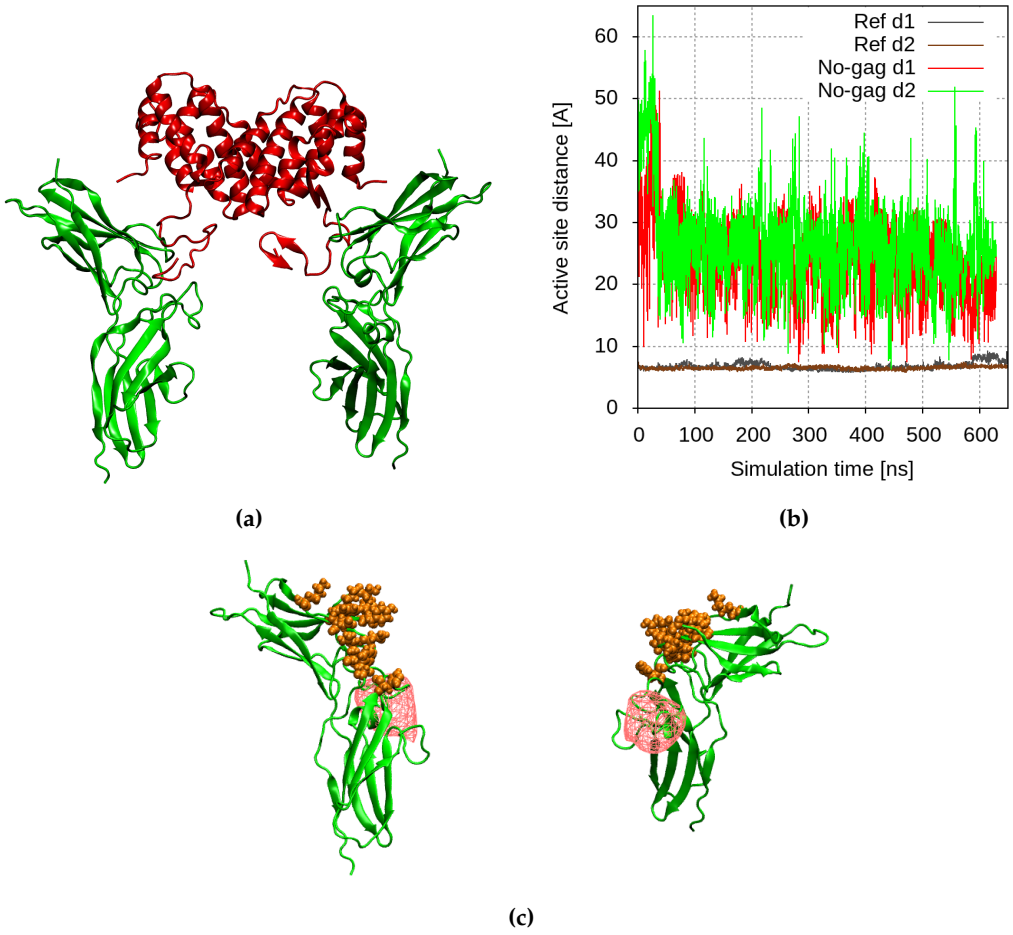

Figure 2. (a) Final conformation of the hIFNγ–hIFNGR1 binding simulation; (b) Time evolution of the COM distances d_1 and d_2 between the binding sites in the hIFNγ and hIFNGR1 molecules without the presence of GAGs; (c) Localized negative charge-density at the "knees" of the two hIFNGR1 subunits, shown in red wireframe, hIFNγ-binding sites are presented in orange spheres.

As seen in Fig. 3, the N-terminal part of hIFNγ monomer A does not form any contacts with chain C of the receptor. Some contacts are formed between the C-terminal part of the B monomer of the cytokine and receptor subunit C, but they do not include the crucial His^{111} and its surrounding residues. As to the other binding interface, the N-termminal part of hIFNγ monomer B does form some contacts with chain D of the receptor, but these are not properly populated and very transient in nature. This is also the case for the interaction of this receptor subunit and the C-terminal part of hIFNγ monomer A (Fig. 4).

These results indicate that the interaction between hIFNγ and hIFNGR1 falls short for an efficient and proper formation of cytokine–receptor complex. A possible reason might be that the overall negative charge of the hIFNGR1 is insufficient for effective attraction

Preprints (www.preprints.org) | NOT PEER-REVIEWED | Posted: 5 July 2022 doi:10.20944/preprints202207.0058.v1

and strong binding of the hIFNγ molecule. Therefore, one might expect that additional negative charges in the vicinity of hIFNGR1 are necessary for the formation of a functional hIFNγ–hIFNGR1 complex.

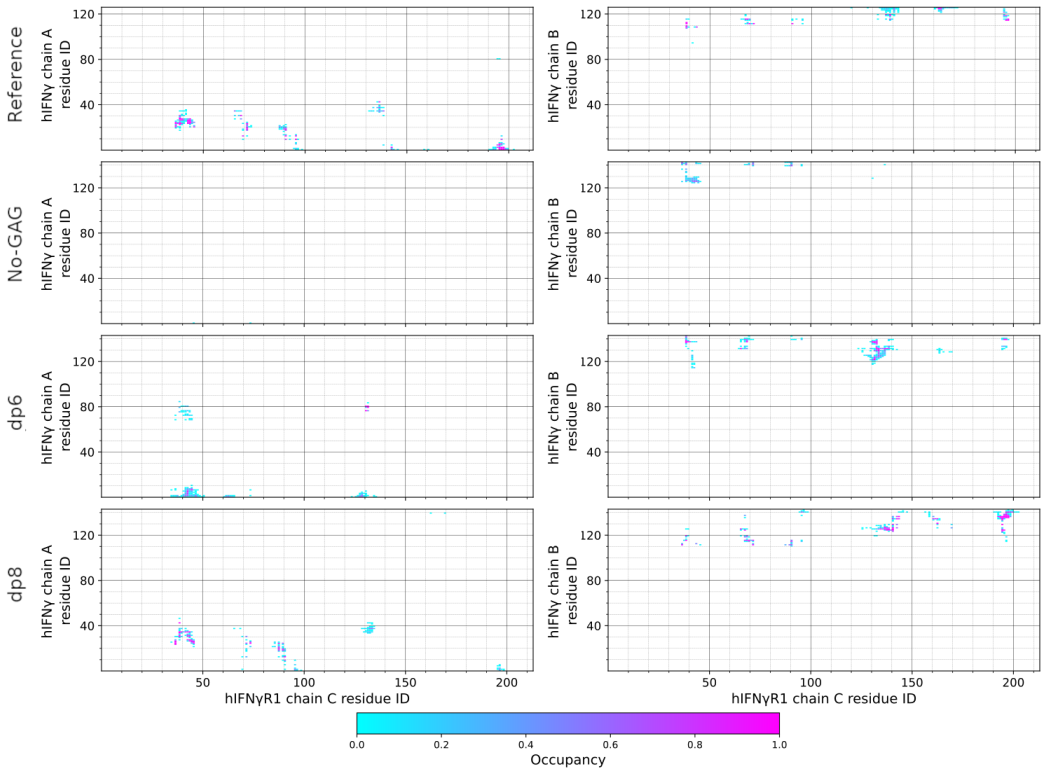

Figure 3. Contact maps between the two hIFNγ monomers (chain A and B) and receptor subunit C.

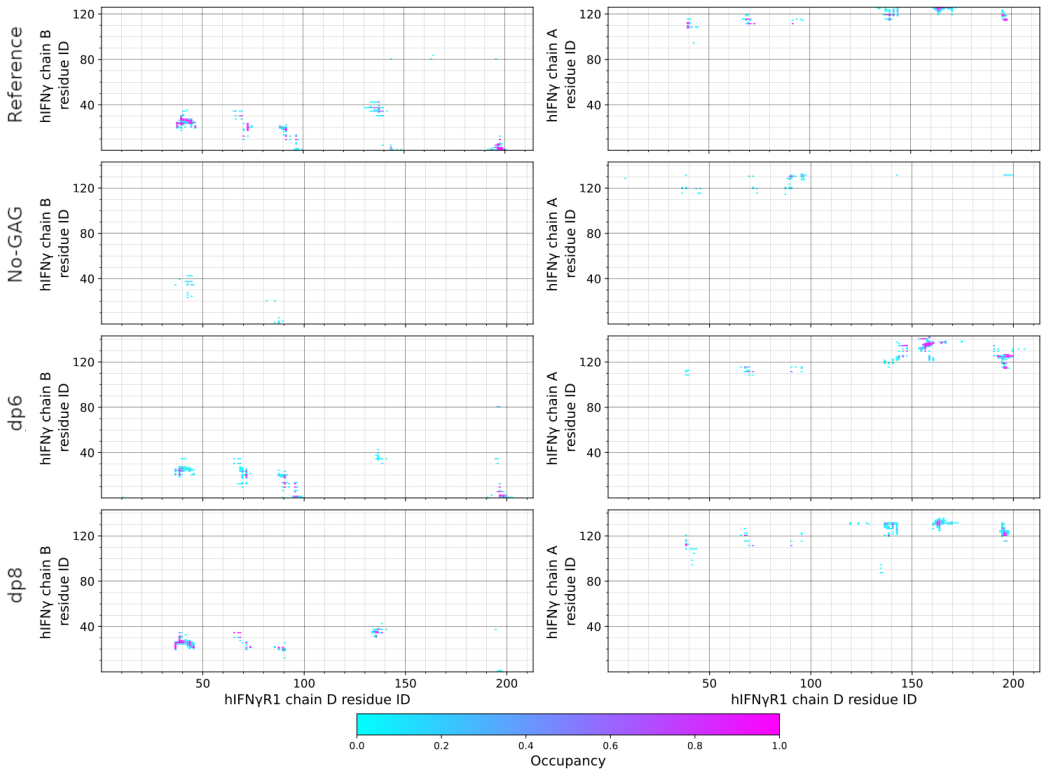

Figure 4. Contact maps between the two hIFNγ monomers (chain B and A) and receptor subunit D.

Preprints (www.preprints.org) | NOT PEER-REVIEWED | Posted: 5 July 2022 doi:10.20944/preprints202207.0058.v1

Based on literature data [23,46], we identified the GAGs heparin and heparan sulfate as appropriate candidates for molecules contributing with their strong negative charges to the formation of a functional hIFNγ— hIFNGR1 complex. Moreover, HS participates in the structure of HSPGs, which are ubiquitous components of basement membranes.

When HS-like oligosaccharides are placed between the two receptor subunits, they attract electrostatically the C-termini of hIFNγ and pull the whole molecule downward in between the receptor molecules. In the dp6 simulation, the carbohydrates are not able to pull the cytokine molecule well enough, so that only one of the two binding interfaces come into proper contact. The hIFNγ globule tilts at one side, so that the other binding site is rotated and not in the vicinity of the second receptor subunit (Fig. 5a,c). This is also evident in Fig. 3 and Fig. 4 (third-row panels) – while the contact maps of hIFNγ and receptor subunit D resembles the reference contact map (Fig. 4), the interface with hIFNGR1 chain C is completely off (Fig. 3).

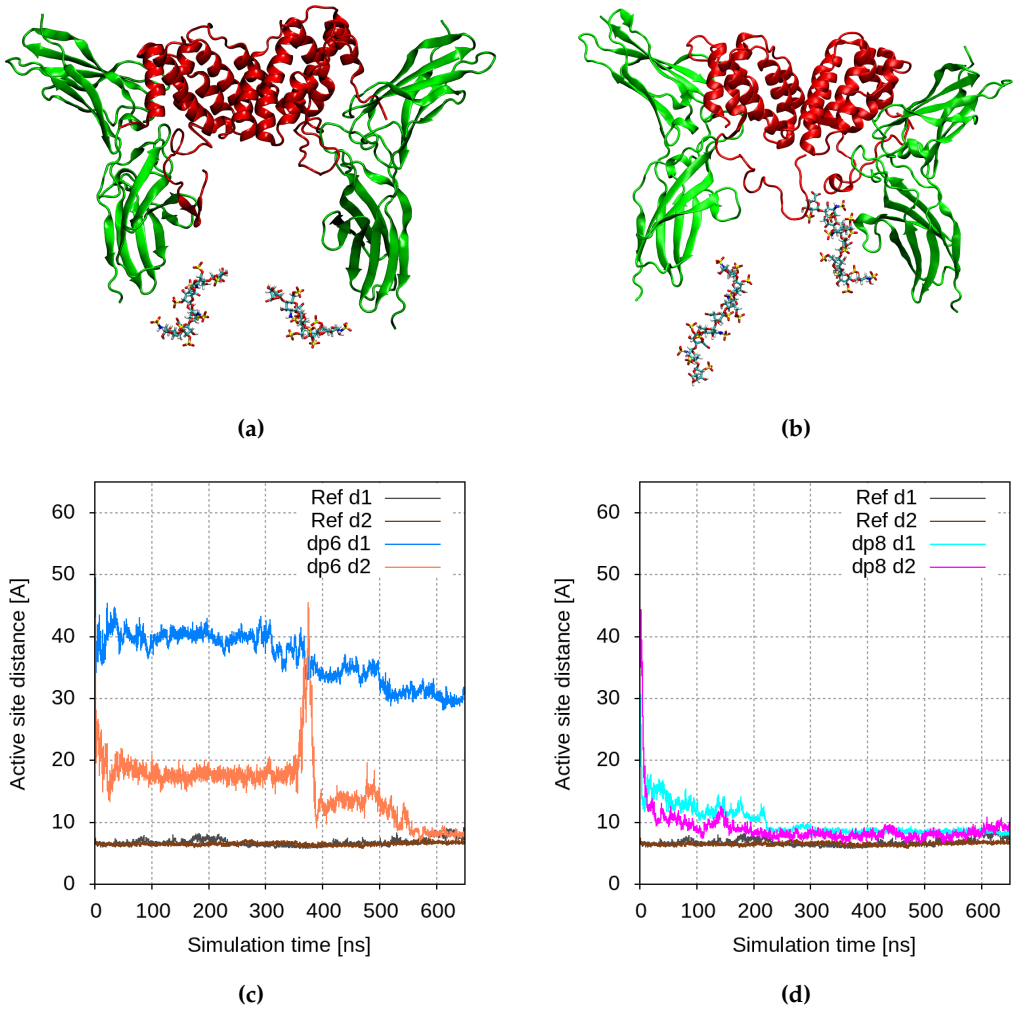

Figure 5. Final conformation of the hIFNγ–hIFNGR1 binding simulation in the presence of (a) hexa-, or (b) octasaccharides; Time evolution of the COM distances d_1 and d_2 between the binding sites in the hIFNγ and hIFNGR1 molecules in the presence of (c) hexa-, or (d) octasaccharides.

When octasaccharides are present between the receptor molecules, they manage to attract the two C-termini of the cytokine much stronger. This interaction is very intense and speedy – within the first 100 ns the whole globule is pulled down between the two receptor subunits (Fig. 5b,d). The contact maps in the lowermost panels in Fig. 3 and Fig. 4 also demonstrate that in this scenario the binding interfaces adjust fairly well to each other and closely resemble the reference contact maps (top panels in Fig. 3 and Fig. 4).

Preprints (www.preprints.org) | NOT PEER-REVIEWED | Posted: 5 July 2022 doi:10.20944/preprints202207.0058.v1

These results allowed us to present a model of hIFNγ–hIFNGR1 interaction according to which two HS molecules (octasaccharides) are located in the "bottom" of the hIFNGR1 receptor unit (corresponding to the basement cell membrane). They attract the hIFNγ unstructured C-termini much stronger than the receptor itself thus participating in the initial stages of cytokine–receptor interaction. As a result, the hIFNγ molecule is pulled downwards to the cell surface, which favors the adoption of a correct (matching the receptor) conformation necessary for the formation of a stable and functional hIFNγ–hIFNGR1 complex.

3.2. Disrupting HSPG Sulfation Decreases the Antiproliferative Activity of hIFNγ

Cell-surface sulfation is mainly due to the presence of proteoglycans on the cellular membrane, in particular heparan sulfate proteoglycans. Therefore, a comparative study of the antiproliferative activity of hIFNγ in normal cell and cells depleted from HSPG sulfation would be indicative of whether GAGs play a key role in the process of cytokine–receptor binding. For this purpose, we measured the antiproliferative activity of hIFNγ in treated with $NaClO_3$ versus non treated cells by modified kynurenine bioassay [44]. For the treated cells, cultured in a media containing $NaClO_3$, we observed significant reduction of the hIFNγ signal indicating an 86% lowered biological activity of the cytokine (Fig. 6). This result emphasizes the role of cell surface sulfation for the interaction of the cytokine with its specific cellular receptor, thus supporting the MD simulation data and confirming qualitatively our hypothesis regarding the co-receptor role of HSPGs in the formation of the hIFNγ–hIFNGR1 complex.

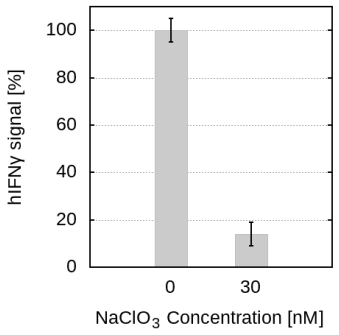

Figure 6. Effect of $NaClO_3$ on the hIFNγ signal. After subtraction of the blank value, the absorbance obtained from cells treated with hIFNγ and cultivated in culture medium containing 30 mM $NaClO_3$ is related to that obtained from cells treated with hIFNγ only, taken as 100%.

4. Discussion

hIFNγ is a signaling molecule, which is essential for both innate and adaptive immunity. It plays a crucial role in the modulation of the immune response against various pathogens, including viruses, bacteria, parasites. However, the activity of hIFNγ is also associated with the pathological development and progression of various autoimmune and neurodegenerative diseases, inflammation and cancer [10,11,16,47]. The development of adequate inhibitors of its actions necessitates proper understanding of how this cytokine actually binds to its extracellular receptor.

Although numerous studies undoubtedly prove the modulating effect of the unstructured C-terminal region on hIFNγ activity, they fail to explain the molecular mechanism of its action. Lortat-Jacob and collaborators were the first to realize that the role of hIFNγ C-terminus could not be explained simply by considering the hIFNγ—hIFNGR1 interaction as a protein-protein event. They published a series of papers clarifying the role of a third, non-protein molecule (highly sulfated oligosaccharides) in this interaction [17–19]. As already discussed, the same research group identified two basic segments (D1 and D2) in the hIFNγ C-terminus, responsible for the specific binding of HS [48] and revealed domains in HS interacting specifically with these two parts of the cytokine [49].

Here we showed computationally that the full-length hIFNγ was unable to form a proper complex with its cell-surface receptor. The above experimental findings paved the way for the present theoretical study on the formation of the hIFNγ–hIFNGR1 complex with HS oligosaccharides being involved in this process, next to the cytokine and its receptor.

The computer simulations described above demonstrate that the formation of a stable hIFNγ—hIFNGR1 complex is a tedious process, unless an additional negatively charged

 doi:10.20944/preprints202207.0058.v1

molecule is present in the vicinity of the hIFNγ receptor. The minimal charge of this molecule should be comparable with the charge of the sample octasaccharide dp8 used in the simulations (-16e) and it must be located in the basement of the hIFNγ receptor unit. We hypothesize that these additional molecules are HSPGs, which are present on almost all cell membranes.

It should be noted, that cell-surface HSPGs are known to serve as co-receptors for various signaling molecules and growth factors [50–52]. HSPGs enhance their ligands' activity by increasing their local concentration, controlling their destination, affecting their conformation, oligomerization state, or stability [50].

Our results suggest that the formation of the cytokine-receptor complex is a multistage tripartite process. In the early stage, the flexible positively charged C-termini of the hIFNγ homodimer navigate the cytokine towards the receptor, being attracted by both negatively charged hIFNGR1 and HSPGs. When in close proximity to the receptor, the cytokine C-termini fall under the stronger influence of the HS electrostatic field that prevents their binding to the hIFNGR1 "knees". At this stage, the flexible C-termini bend and pull downward the globular part of hIFNγ. When the positive charges of D1 and D2 are neutralized by HS chains, and the globular part of hIFNγ is properly situated in the cliff of hIFNGR1 receptor, the cytokine-receptor binding interfaces are positioned close to each other, which provides for proper formation of the complex.

Our experimental data also indirectly supports this hypothesis. Inhibition of HSPG sulfation by sodium chlorate leads to reduction of hIFNγ biological activity by more than 80%. We speculate that this drastic activity decrease is due to hindered receptor binding because of damaged co-receptor structure. In [53] it was experimentally confirmed, that hIFNγ also interacts with another GAG – chondroitin sulfate and its proteoglycans. Chondroitinase treatment of cells led to a more than 50% reduction in hIFNγ binding, and pretreatment with the enzyme significantly reduced cellular response to the cytokine. Recently, it was found that coating cells with heparin/collagen layers increases cellular response to hIFNγ, especially when the top layer was heparin [54]. These findings provide further basis for the asserted key role that HS chains play in the formation of the hIFNγ-hIFNGR1 complex.

The proposed here model explains well the inhibitory effect of exogenous sulfated octasaccharides (such as dp8) on hIFNγ activity considered in a certain context in [55], as well as the decrease or complete loss of biological activity in constructs containing very short unstructured C-termini [15,56,57]. In the first case the negatively charged molecules neutralize the C-terminal positive charges (i.e. they compete with the endogenous sulfated oligosaccharides fixed on the cell membrane). In the second case, the deep truncation of the C-terminus is accompanied by removal of positive charges, which are necessary for the early stages of hIFNγ–hIFNGR1 interaction. The negative effect of the C-terminal shortening on hIFNγ biological activity is better expressed when the truncation affects the positively charged domain D1.

As mentioned above, the gradual truncation of the hIFNγ C-terminus has a two-phase effect on hIFNγ activity. We are tempted to explain the (up to 10 times) higher biological activity of hIFNγ constructs containing 6-7 aa shorter C-termini by some advantages of the shorter unstructured C-terminal tail [16]. Even after removal of 6-7 aa (including domain D2), the hIFNγ C-terminus still carries enough positive charges (mainly on account of domain D1) to recognize the hIFNGR1 receptor, to initiate hIFNγ—hIFNGR1 binding and to decrease the probability for interaction of the C-terminus with the "knee" of hIFNGR1. The smaller size of partly truncated C-termini (probably) fits better the limited space of the hIFNGR1 cliff, thus favoring the adoption of better hIFNγ conformation, necessary for the formation of a more stable hIFNγ—hIFNGR1 complex as compared to the full-size (143 aa) hIFNγ. We tend to disagree with Lortat-Jacob et al. [49] explaining the higher activity of truncated hIFNγ preparations with the competition of the two D1 and D2 domains for the same binding site in the hIFNGR1 subunit.

 doi:10.20944/preprints202207.0058.v1

5. Conclusions

Molecular dynamics simulations are carried out to investigate the intimate mechanism of hIFNγ–hIFNGR1 interaction. As a result, a multistage model of hIFNγ–hIFNGR1 complex formation is proposed, with heparan sulfate proteoglycans playing a key process-promoting role as a hIFNγ co-receptor. The negatively charged sulfated oligosaccharides bind the positively charged C-termini thus facilitating the proper positioning of the globular part of hIFNγ with respect to the hIFNGR1. Experimental data supports the proposed model.

Author Contributions: Conceptualization, L.L.; experimental design, G.N.; computational methodology, P.P., E.L., and E.M.; simulations, E.M., P.P., and E.L.; experimental set up, E.K., K.M.; validation (computing), E.M., P.P., and L.L.; validation (experiments), G.N., E.K.; formal analysis, all authors; investigation, all authors; laboratory resources, G.N.; computational resources, L.L., N.I.; data curation, E.M., P.P., E.K.; writing—original draft preparation, E.L., E.K.; writing—review and editing, N.I., L.L., and G.N.; visualization, P.P., E.L.; supervision, L.L., G.N.; project administration, G.N., N.I.; funding acquisition, L.L., G.N. All authors have read and agreed to the published version of the manuscript.

Funding: This work was supported in part by the Bulgarian National Science Fund under Grants DN-11/20/2017 and KP-06-DK1/5/2021 SARSSIM.

Acknowledgments: Computational resources were provided by BioSim HPC cluster at the Faculty of Physics, Sofia University "St. Kliment Ohridski", the Centre for Advanced Computing and Data Processing, supported under Grant BG05M2OP001-1.001-0003 by the Science and Education for Smart Growth Operational Program (2014-2020) and co-financed by the European Union through the European structural and investment funds and by CI TASK (Centre of Informatics – Tricity Academic Supercomputer & networK), Gdansk (Poland).

Conflicts of Interest: The authors declare no conflict of interest. The funders had no role in the design of the study; in the collection, analyses, or interpretation of data; in the writing of the manuscript, or in the decision to publish the results.

Abbreviations

The following abbreviations are used in this manuscript:

aa	Amino acid
dp	Degree of polymerization
GAG	Glycosaminoglycans
hIFNγ	Human interferon-gamma
hIFNGR	Human interferon-gamma receptor
hIFNGR1	Human interferon-gamma receptor chain-1
hIFNGR2	Human interferon-gamma receptor chain-2
HS	Heparan sulfate
HSPG	Heparan sulfate proteoglycan
IFNγ	Interferon-gamma
MD	Molecular dynamics

References

1. Pestka, S.; Krause, C.D.; Walter, M.R. Interferons, interferon-like cytokines, and their receptors. *Immunological Reviews* **2004**, *202*, 8–32.
2. Tsanev, R.G.; Ivanov, I. *Immune Interferon: Properties and Clinical Applications*; CRC Press, 2001.
3. Farrar, M.A.; Schreiber, R.D. The molecular cell biology of interferon-gamma and its receptor. *Annual review of immunology* **1993**, *11*, 571–611.
4. Schroder, K.; Hertzog, P.J.; Ravasi, T.; Hume, D.A. Interferon-γ: an overview of signals, mechanisms and functions. *Journal of Leukocyte Biology* **2004**, *75*, 163–189.
5. Greenlund, A.; Farrar, M.; Viviano, B.; Schreiber, R. Ligand-induced IFN gamma receptor tyrosine phosphorylation couples the receptor to its signal transduction system (p91). *The EMBO Journal* **1994**, *13*, 1591–1600.
6. Bach, E.A.; Aguet, M.; Schreiber, R.D. THE IFNγ RECEPTOR:A Paradigm for Cytokine Receptor Signaling. *Annual Review of Immunology* **1997**, *15*, 563–591.

7. Ealick, S.E.; Cook, W.J.; Vijay-Kumar, S.; Carson, M.; Nagabhushan, T.L.; Trotta, P.P.; Bugg, C.E. Three-dimensional structure of recombinant human interferon-γ. *Science* **1991**, *252*, 698–702.
8. Walter, M.R.; Windsor, W.T.; Nagabhushan, T.L.; Lundell, D.J.; Lunn, C.A.; Zauodny, P.J.; Narula, S.K. Crystal structure of a complex between interferon-gamma and its soluble high-affinity receptor. *Nature* **1995**, *376*, 230–235.
9. Thiel, D.; le Du, M.H.; Walter, R.; D'Arcy, A.; Chène, C.; Fountoulakis, M.; Garotta, G.; Winkler, F.; Ealick, S. Observation of an unexpected third receptor molecule in the crystal structure of human interferon-γ receptor complex. *Structure* **2000**, *8*, 927–936.
10. Rinderknecht, E.; O'Connor, B.H.; Rodriguez, H. Natural human interferon-gamma. Complete amino acid sequence and determination of sites of glycosylation. *The Journal of biological chemistry* **1984**, *259*, 6790–6797.
11. Pan, Y.C.E.; Stern, A.S.; Familletti, P.C.; Chizzonite, R.; Khan, F.R. Structural characterization of human interferon γ Heterogeneity of the carboxyl terminus. *European Journal of Biochemistry* **1987**, *166*, 145–149.
12. Haelewyn, J.; Michiels, L.; Verhaert, P.; Hoylaerts, M.F.; Witters, R.; De Ley, M. Interaction of truncated human interferon gamma variants with the interferon gamma receptor: crucial importance of Arg-129. *Biochemical Journal* **1997**, *324*, 591–595.
13. Schein, C.; Haugg, M. Deletions at the C-terminus of interferon gamma reduce RNA binding and activation of double-stranded-RNA cleavage by bovine seminal ribonuclease. *The Biochemical journal* **1995**, *307*, 123–127.
14. Lundell, D.; Lunn, C.; Senior, M.; Zavodny, P.; Narula, S. Importance of the loop connecting A and B helices of human interferon-gamma in recognition by interferon-gamma receptor. *Journal of Biological Chemistry* **1994**, *269*, 16159–16162.
15. Döbeli, H.; Gentz, R.; Jucker, W.; Garotta, G.; Hartmann, D.; Hochuli, E. Role of the carboxy-terminal sequence on the biological activity of human immune interferon (IFN-γ). *Journal of Biotechnology* **1988**, *7*, 199–216.
16. Nacheva, G.; Todorova, K.; Boyanova, M.; Berzal-Herranz, A.; Karshikoff, A.; Ivanov, I. Human Interferon gamma: significance of the C-terminal flexible domain for its biological activity. *Archives of Biochemistry and Biophysics* **2003**, *413*, 91–98.
17. Lortat-Jacob, H. Interferon and heparan sulphate. *Biochemical Society Transactions* **2006**, *34*, 461–464.
18. Lortat-Jacob, H.; Brisson, C.; Guerret, S.; Morel, G. Non-receptor-mediated tissue localization of human interferon-gamma: role of heparan sulfate/heparin-like molecules. *Cytokine* **1996**, *8*, 557–566.
19. Sadir, R.; Forest, E.; Lortat-Jacob, H. The heparan sulfate binding sequence of interferon-gamma increased the on rate of the interferon-gamma-interferon-gamma receptor complex formation. *The Journal of biological chemistry* **1998**, *273*, 10919–10925.
20. Couchman, J.R. Heterogeneous distribution of a basement membrane heparan sulfate proteoglycan in rat tissues. *Journal of Cell Biology* **1987**, *105*, 1901–1916.
21. de Boeck, H.; Lories, V.; David, G.; Cassiman, J.J.; van den Berghe, H. Identification of a 64 kDa heparan sulphate proteoglycan core protein from human lung fibroblast plasma membranes with a monoclonal antibody. *The Biochemical journal* **1987**, *247*, 765–771.
22. Sarrazin, S.; Lamanna, W.C.; Esko, J.D. Heparan Sulfate Proteoglycans. *Cold Spring Harbor perspectives in biology* **2011**, *3*, a004952.
23. Lortat-Jacob, H.; Kleinman, H.K.; Grimaud, J.A. High-affinity binding of interferon-gamma to a basement membrane complex (matrigel). *The Journal of Clinical Investigation* **1991**, *87*, 878–883.
24. Vanhaverbeke, C.; Simorre, J.P.; Sadir, R.; Gans, P.; Lortat-Jacob, H. NMR characterization of the interaction between the C-terminal domain of interferon-γ and heparin-derived oligosaccharides. *Biochemical Journal* **2004**, *384*, 93–99.
25. Berman, H.M.; Westbrook, J.; Feng, Z.; Gilliland, G.; Bhat, T.N.; Weissig, H.; Shindyalov, I.N.; Bourne, P.E. The Protein Data Bank. *Nucleic Acids Research* **2000**, *28*, 235–242.
26. Petkov, P.; Lilkova, E.; Ilieva, N.; Nacheva, G.; Ivanov, I.; Litov, L. Computational Modelling of the Full Length hIFN-γ Homodimer. In Proceedings of the Large-Scale Scientific Computing 2017; Lirkov, I.; Margenov, S., Eds. Springer International Publishing, 2018, pp. 544–551.
27. Lilkova, E.; Petkov, P.; Ilieva, N.; Krachmarova, E.; Nacheva, G.; Litov, L. Molecular modeling of the effects of glycosylation on the structure and dynamics of human interferon-gamma. *Journal of Molecular Modeling* **2019**, *25*, 127.
28. Emsley, P.; Cowtan, K. *Coot*: model-building tools for molecular graphics. *Acta Crystallographica Section D* **2004**, *60*, 2126–2132.

29. Park, S.J.; Lee, J.; Qi, Y.; Kern, N.R.; Lee, H.S.; Jo, S.; Joung, I.; Joo, K.; Lee, J.; Im, W. CHARMM-GUI Glycan Modeler for modeling and simulation of carbohydrates and glycoconjugates. *Glycobiology* **2019**, *29*, 320–331.
30. Jo, S.; Kim, T.; Iyer, V.G.; Im, W. CHARMM-GUI: A web-based graphical user interface for CHARMM. *Journal of Computational Chemistry* **2008**, *29*, 1859–1865.
31. Guvench, O.; Mallajosyula, S.S.; Raman, E.P.; Hatcher, E.; Vanommeslaeghe, K.; Foster, T.J.; Jamison, F.W.; MacKerell, A.D. CHARMM Additive All-Atom Force Field for Carbohydrate Derivatives and Its Utility in Polysaccharide and Carbohydrate–Protein Modeling. *Journal of Chemical Theory and Computation* **2011**, pp. 3162–3180.
32. Case, D.; Betz, R.; Cerutti, D.; T.E. Cheatham, I.; Darden, T.; Duke, R.; Giese, T.; Gohlke, H.; Goetz, A.; Homeyer, N.; et al. AMBER 2016. University of California, San Francisco, 2016. https://ambermd.org/AmberTools.php.
33. Abraham, M.J.; Murtola, T.; Schulz, R.; Páll, S.; Smith, J.C.; Hess, B.; Lindahl, E. GROMACS: High performance molecular simulations through multi-level parallelism from laptops to supercomputers. *SoftwareX* **2015**, *1-2*, 19 – 25.
34. Huang, J.; Rauscher, S.; Nawrocki, G.; Ran, T.; Feig, M.; de Groot, B.L.; Grubmüller, H.; MacKerell Jr, A.D. CHARMM36m: an improved force field for folded and intrinsically disordered proteins. *Nature Methods* **2016**, *14*, 71–73.
35. Berendsen, H.J.C.; Postma, J.P.M.; van Gunsteren, W.F.; DiNola, A.; Haak, J.R. Molecular dynamics with coupling to an external bath. *The Journal of Chemical Physics* **1984**, *81*, 3684.
36. Bussi, G.; Donadio, D.; Parrinello, M. Canonical sampling through velocity rescaling. *The Journal of chemical physics* **2007**, *126*, 014101.
37. Parrinello, M.; Rahman, A. Crystal Structure and Pair Potentials: A Molecular-Dynamics Study. *Physical Review Letters* **1980**, *45*, 1196.
38. Parrinello, M.; Rahman, A. Polymorphic transitions in single crystals: A new molecular dynamics method. *Journal of Applied Physics* **1981**, *52*, 7182.
39. Hockney, R.; Goel, S.; Eastwood, J. Quiet high-resolution computer models of a plasma. *Journal of Computational Physics* **1974**, *14*, 148 – 158.
40. Hess, B. P-LINCS: A Parallel Linear Constraint Solver for Molecular Simulation. *Journal of Chemical Theory and Computation* **2008**, *4*, 116–122.
41. Essmann, U.; Perera, L.; Berkowitz, M.L.; Darden, T.; Lee, H.; Pedersen, L.G. A smooth particle mesh Ewald method. *The Journal of Chemical Physics* **1995**, *103*, 8577–8593.
42. Sadir, R.; Lortat-Jacob, H.; Morel, G. Internalization and Nuclear Translocation of IFN-γ and IFN-γR: an Ultrastructural Approach. *Cytokine* **2000**, *12*, 711–714.
43. Tileva, M.; Krachmarova, E.; Ivanov, I.; Maskos, K.; Nacheva, G. Production of aggregation prone human interferon gamma and its mutant in highly soluble and biologically active form by SUMO fusion technology. *Protein Expression and Purification* **2016**, *117*, 26–34.
44. Boyanova, M.; Tsanev, R.; Ivanov, I. A modified kynurenine bioassay for quantitative determination of human interferon-γ. *Analytical Biochemistry* **2002**, *308*, 178–181.
45. McGibbon, R.T.; Beauchamp, K.A.; Harrigan, M.P.; Klein, C.; Swails, J.M.; Hernández, C.X.; Schwantes, C.R.; Wang, L.P.; Lane, T.J.; Pande, V.S. MDTraj: A Modern Open Library for the Analysis of Molecular Dynamics Trajectories. *Biophysical Journal* **2015**, *109*, 1528 – 1532.
46. Lortat-Jacob, H.; Baltzer, F.; Grimaud, J.A. Heparin Decreases the Blood Clearance of Interferon-γ and Increases Its Activity by Limiting the Processing of Its Carboxyl-terminal Sequence. *Journal of Biological Chemistry* **1996**, *271*, 16139 – 16143.
47. Xu, K.; Jin, L. The role of heparin/heparan sulphate in the IFN-γ-led Arena. *Biochimie* **2020**, *170*, 1–9.
48. Hugues, L.J.; Grimaud, J.A. Interferon-γ binds to heparan sulfate by a cluster of amino acids located in the C-terminal part of the molecule. *FEBS Letters* **1991**, *280*, 152–154.
49. Lortat-Jacob, H.; Turnbull, J.E.; Grimaud, J.A. Molecular organization of the interferon γ-binding domain in heparan sulphate. *Biochemical Journal* **1995**, *310*, 497–505.
50. Hayashida, K.; Aquino, R.S.; Park, P.W. Coreceptor functions of cell surface heparan sulfate proteoglycans. *American Journal of Physiology-Cell Physiology* **2022**, *322*, C896–C912.
51. Hassan, N.; Greve, B.; Espinoza-Sánchez, N.A.; Götte, M. Cell-surface heparan sulfate proteoglycans as multifunctional integrators of signaling in cancer. *Cellular Signalling* **2021**, *77*, 109822.
52. Collins, L.E.; Troeberg, L. Heparan sulfate as a regulator of inflammation and immunity. *Journal of Leukocyte Biology* **2019**, *105*, 81–92.
53. Hurt-Camejo, E.; Rosengren, B.; Sartipy, P.; Elfsberg, K.; Camejo, G.; Svensson, L. CD44, a Cell Surface Chondroitin Sulfate Proteoglycan, Mediates Binding of Interferon-γ and Some of Its

 doi:10.20944/preprints202207.0058.v1

Biological Effects on Human Vascular Smooth Muscle Cells*. *Journal of Biological Chemistry* **1999**, *274*, 18957–18964.

54. Castilla-Casadiego, D.A.; García, J.R.; García, A.J.; Almodovar, J. Heparin/Collagen Coatings Improve Human Mesenchymal Stromal Cell Response to Interferon Gamma. *ACS Biomaterials Science & Engineering* **2019**, *5*, 2793–2803.
55. Perez Sanchez, H.; Tatarenko, K.; Nigen, M.; Pavlov, G.; Imberty, A.; Lortat-Jacob, H.; Garcia de la Torre, J.; Ebel, C. Organization of human interferon gamma-heparin complexes from solution properties and hydrodynamics. *Biochemistry* **2006**, *45*, 13227–13238.
56. Wetzel, R.; Perry, L.J.; Veilleux, C.; Chang, G. Mutational analysis of the C-terminus of human interferon-γ. *Protein Engineering, Design and Selection* **1990**, *3*, 611–623.
57. de la Maza, L.; Peterson, E.; Burton, L.; Gray, P.; Rinderknecht, E.; Czarniecki, C. The antichlamydial, antiviral, and antiproliferative activities of human gamma interferon are dependent on the integrity of the C terminus of the interferon molecule. *Infection and immunity* **1987**, *55*.